DOI: 10.61782/fa.2023.0177

forum acusticum 2023

SOUND PRESSURE RADIATED BY A POINT-SOURCE IN ARBITRARY MOTION ABOVE AN ABSORBING GROUND. APPLICATION TO AIRCRAFT NOISE.

Bill Kayser **Didier Dragna** **Philippe Blanc-Benon**

Univ Lyon, Ecole Centrale de Lyon, CNRS, Univ Claude Bernard Lyon 1, INSA Lyon, LMFA, UMR5509, 69130, Ecully, France

ABSTRACT

The acoustic regulations are increasingly stringent for aircraft noise. Aircraft manufacturers must therefore be able to predict accurately aircraft noise for certification scenarios as early as the design phase. Acoustic propagation models used in the industry are however based on simplified approaches. Thus, we use a heuristic model for a point source in arbitrary motion in a homogeneous atmosphere at rest above an absorbing ground proposed in the literature. It removes most of the simplification of existing approaches, but has however not been validated and applied for aircraft noise. These are the two goals of this study. The heuristic expression is first validated satisfactorily for several test cases against a numerical solution from a time-domain solver of the Linearized Euler equations. Then, a parametric study on ground properties (i.e. absorption, thickness and roughness) is performed to analyze ground effects on sound pressure levels estimation.

Keywords: Aircraft noise, heuristic formulation, ground effects.

1. INTRODUCTION

Aircraft exterior noise measurements for certification purposes must be acquired by microphones placed at 1.2 m above the ground. Such procedure yields a characteristic comb filtering effect. This method is thus really sensitive to ground properties, which can lead to high uncertainty on SPL measurements, especially for single tones. Recently, there is an on-going effort within the Committee on Aviation Environmental Protection to define improved noise measurement methods for use in noise certification testing of civil airplanes, *e.g.* [1, 2]. The use of numerical method can help design new aircraft noise control standards. However, existing engineering models for predicting outdoor aircraft noise use a simplified approach by considering a quasi-stationary point source in homogeneous atmosphere. Such hypothesis is not valid for sources travelling at a non-negligible Mach number in outdoor environment, which is the case for the context of aircraft noise. The improvement of existing prediction methods is thus a major key point to reduce aircraft noise prediction uncertainties.

The present work aims at improving the modelling of aircraft noise propagation by using a heuristic model for a point source in arbitrary motion [3]. This heuristic model can be seen as an extension of the analytical "Dopplerized" Weyl Van der Pol formulation [4–8] that is only valid for sources in motion parallel to the ground. The heuristic model does not yet account for the effects of the atmosphere on sound propagation (refraction and scattering), but does consider ground effects (absorption and scattering by ground roughness) where the ground admittance is determined at the Doppler frequencies [9–11].

This study aims at validating the heuristic expression by using a reference research model based on a three-dimensional (3D) Finite Difference Time Domain (FDTD) techniques that solves the linearized Euler equations [12]. Lastly, a parametric study on ground properties

*__Corresponding author__: bill.kayser@ec-lyon.fr.

is performed to quantify ground effects on sound pressure level (SPL) in the context of aircraft noise.

The paper is organised as follows. Sec. 2 presents the heuristic formulation. Then, the comparison against the 3D FDTD solution is performed in Sec. 3. Sec. 4 presents the parametric study on ground properties. Finally, conclusions are given in Sec. 5.

2. SOUND FIELD FORMULATION FOR A MOVING POINT SOURCE IN A HOMOGENEOUS MEDIUM ABOVE A GROUND

This section gives the theoretical basis of sound propagation for a point source moving above an absorbing ground, for both a rectilinear motion and an arbitrary motion.

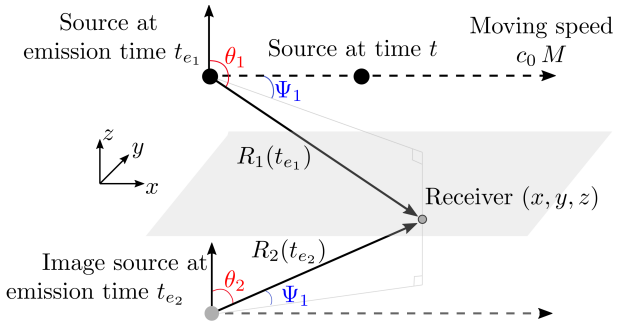

Figure 1. Geometry considered for a moving point source in rectilinear motion above the ground.

Fig. 1 presents the geometry of the problem considered when the source is moving at constant speed and height above the ground. The subscripts $_1$ and $_2$ refer respectively to the direct and reflected waves. The angles θ and Ψ are respectively the polar angle and the azimuth angle of the sound wave propagation path. The acoustic path length at the corresponding emission time t_e (Eqs. (11) and (13)) is denoted by R (Eq. (12)). The sound speed is c_0.

2.1 Formulation

An omnidirectional point source moving above a flat ground surface is considered. The atmosphere is homogeneous and at rest. The governing equations are the linearized Euler equations:

$$\frac{\partial p}{\partial t} + \rho_0 c_0^2 \nabla \cdot \mathbf{v} = S_0\, \mathrm{e}^{-\mathrm{i}\omega_0 t}\delta[\mathbf{x} - \mathbf{x}_s(t)], \tag{1}$$

$$\frac{\partial \mathbf{v}}{\partial t} + \frac{1}{\rho_0}\nabla p = 0. \tag{2}$$

where p and $\mathbf{v}$ are the acoustic pressure and velocity and $\mathbf{x}_s(t) = (x_s(t), y_s(t), z_s(t))$ denotes the source position. The air density is ρ_0, t is time, and $\mathbf{x} = (x, y, z)$ are the Cartesian coordinates. Note that the source amplitude S_0 is set to 1 Pa s^{-1} m^3 and is omitted in the following for simplicity. The boundary condition at $z = 0$ is given by:

$$v_z + [\tilde{\beta} * p] = 0, \tag{3}$$

where $\tilde{\beta}$ is the inverse Fourier transform of the ground admittance $\beta(\omega)$ and $*$ is the convolution.

2.2 Analytical solution for a point source moving at constant speed and height

We first limit the study to a point source moving at a constant speed and height. Without loss of generality, the source position is chosen as $\mathbf{x}_s = (Mc_0t, 0, z_S)$, where M is the source Mach number. An analytical solution is available for this case [8]. We use in the following an approximate solution [3, 13]. In acoustic far-field, the pressure field can be written as:

$$p = -\frac{\mathrm{i}\omega_0 \mathrm{e}^{-\mathrm{i}\omega_0 t}}{4\pi}\left[\frac{\mathrm{e}^{\mathrm{i}k_0 R_1}}{R_1(1-M_{r_1})^2} + \mathcal{Q}\frac{\mathrm{e}^{\mathrm{i}k_0 R_2}}{R_2(1-M_{r_2})^2}\right], \tag{4}$$

where $k_0 = \omega/c_0$ is the wave number,

$$\mathcal{Q} = \mathcal{R} + (1-\mathcal{R})F(d/\sqrt{1-M_{r_2}}), \tag{5}$$

is the spherical wave reflection coefficient,

$$F(u) = 1 + \mathrm{i}u\sqrt{\pi}w(u) \tag{6}$$

is the boundary loss factor, w is the Faddeeva function,

$$\mathcal{R} = \frac{\cos\theta_2 - \beta(\omega_{e_2})}{\cos\theta_2 + \beta(\omega_{e_2})}, \tag{7}$$

is the plane wave reflection coefficient, $\omega_{e_2} = \omega_0/\sqrt{1-M_{r_2}}$ is the Doppler frequency,

$$d = \frac{1}{2}(1+\mathrm{i})\sqrt{k_0 R_2}(\cos\theta_2 + \beta(\omega_{e_2})), \tag{8}$$

is the numerical distance and

$$M_{r_1} = M \sin\theta_1 \cos\Psi_1, \tag{9}$$
$$M_{r_2} = M \sin\theta_2 \cos\Psi_2, \tag{10}$$

are the Mach number components in the source-receiver directions. This expression is often called the "Doppler-ized" Weyl Van der Pol formulation.

In this expression, geometric quantities must be expressed as a function of emission time t_e. Indeed, the sound received by the receiver at time t has been emitted at time t_e:

$$t_e = t - R(t_e)/c_0, \tag{11}$$

where $R(t) = |\mathbf{x} - \mathbf{x}_s(t)|$ is the source-receiver distance. This leads to:

$$R(t_e) = \sqrt{(x - Mc_0t_e)^2 + y^2 + (z \pm z_s)^2}. \tag{12}$$

The emission time is then determined by solving a polynomial equation of degree 2 in t_e. The physical solution leads to:

$$t_e = \frac{c_0 t - Mx - \sqrt{x^2 + (1-M^2)[y^2 + (z \pm z_s)^2]}}{c_0(1-M^2)}. \tag{13}$$

2.3 Heuristic formulation for a point source in arbitrary motion

Fig. 2 illustrates the case study of a point source moving above a ground in arbitrary motion.

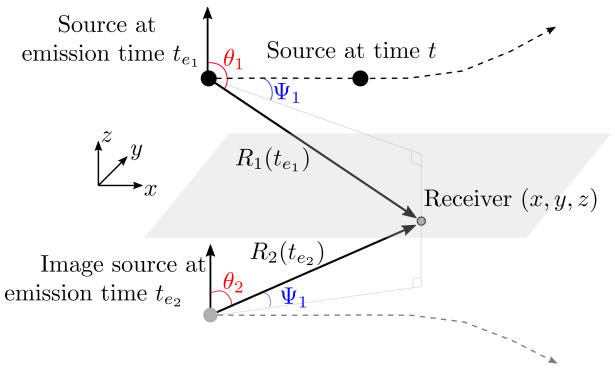

Figure 2. Geometry considered for a moving point source in arbitrary motion above the ground.

For an arbitrary motion, an analytical solution is available in free-field (see, e.g., [4]). However, there is no explicit solution in the literature for a source in an arbitrary motion above an absorbing ground. An heuristic formulation has been proposed in [14], that extends Eq. (4):

$$p = -\frac{\mathrm{i}\omega_0 \mathrm{e}^{-\mathrm{i}\omega_0 t}}{4\pi}\left[\left(1 - M_{r_1} + \frac{\mathrm{i}\dot{M}_{r_1}}{\omega_0}\right)\frac{\mathrm{e}^{\mathrm{i}k_0 R_1}}{R_1(1-M_{r_1})^3} + \mathcal{Q}\left(1 - M_{r_2} + \frac{\mathrm{i}\dot{M}_{r_2}}{\omega_0}\right)\frac{\mathrm{e}^{\mathrm{i}k_0 R_2}}{R_2(1-M_{r_2})^3}\right], \tag{14}$$

where $\dot{M}_r = \frac{\partial M_r}{\partial t_e}$ is the acceleration term in the source-receiver direction.

3. VALIDATION OF THE HEURISTIC FORMULATION WITH A 3D FDTD MODEL

This section proposes a validation of the heuristic formulation with a reference model based on a 3D time-domain solver of the linearized Euler equations. The validation is performed at a small space scale given that the 3D FDTD simulations are expensive in terms of memory and calculation duration. The following analysis considers a rigid ground, as well as a natural absorbing ground called *long-grass*.

3.1 Principles of FDTD model

The linearized Euler equations in Eqs. (1)-(2) are solved using high-order finite-difference time-domain techniques [12, 15]. A broadband impedance boundary condition is implemented at the ground [16]. The sides and the top of the domain also feature a PML layer [17] to prevent unwanted reflections from the limits of the domain.

Instead of the Dirac delta function in the right-hand side of Eq. (1), the source in the FDTD model has a Gaussian spatial distribution:

$$S(\mathbf{x}) = \frac{1}{\pi^{3/2}B^3}\exp\left(-\frac{|\mathbf{x}|^2}{B^2}\right). \tag{15}$$

Note that $S(\mathbf{x})$ tends to the Dirac delta function as B tends to zero. As discussed in [9], the directivity of the Gaussian source is modified by its motion.

For comparison with the heuristic solution, the direct and reflected waves in (14) are multiplied by the directivity of the Gaussian source, which gives:

$$p = -\frac{\mathrm{i}\omega_0 \mathrm{e}^{-\mathrm{i}\omega_0 t}}{4\pi}\left[\frac{\mathrm{e}^{\mathrm{i}k_0 R_1}}{R_1(1-M_{r_1})^2}\exp\left(-\frac{k_0^2 B^2}{4(1-M_{r_1})^2}\right) + \mathcal{Q}\frac{\mathrm{e}^{\mathrm{i}k_0 R_2}}{R_2(1-M_{r_2})^2}\exp\left(-\frac{k_0^2 B^2}{4(1-M_{r_2})^2}\right)\right]. \quad (16)$$

3.2 The case study and the results

The validation is performed in a 3D propagation domain of size (110, 10, 7) m. The mesh grid is uniform and the grid step is equal to 0.1 m. The width of the Gaussian source is chosen as $B = 0.36$ m. The PML thickness is set to 3 m. The source is initially placed at the location (0, 0, 2) m and is moving at constant speed and height along the x-direction as illustrated in Fig. 3.

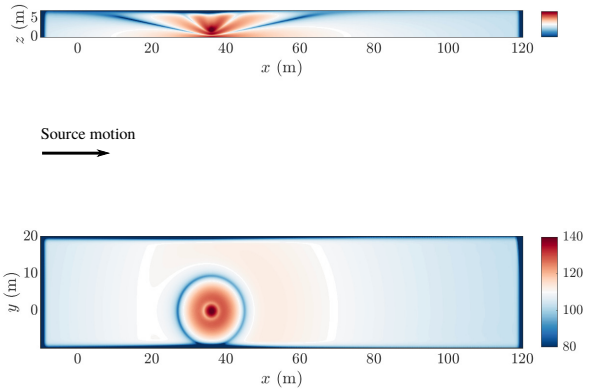

Figure 3. Example of SPL maps obtained with the 3D FDTD model. The frequency is $f = 200$ Hz, the ground is rigid, and the source Mach number is $M = 0.3$.

The next sections provide results for both rigid and natural grounds. The rigid ground corresponds to $\beta = 0$, which leads to $\mathcal{Q} = 1$. The *long-grass* ground is considered through the *Slit pore* ground impedance model [18] with porosity $\Omega = 0.76$, tortuosity $T = \Omega^{0.5}$ and airflow resistivity set to 71.7 kPa s m^{-2}.

3.2.1 *Rigid ground*

Fig. 4 shows an excellent agreement between the FDTD modelling and the heuristic simulations, for both $f = 50$ Hz and 500 Hz. The results at the receiver (40, 0, 5) m highlight strong interference patterns that are induced by the reflected waves on the *rigid* ground. The convective amplification effect is visible as pressure amplitude is different when the source approaches the receiver ($t - x_r/u < 0$) than when it recedes from the receiver ($t - x_r/u > 0$). In addition, the Doppler effect leads to the shift in the interference pattern on both sides of $t - x_r/u = 0$.

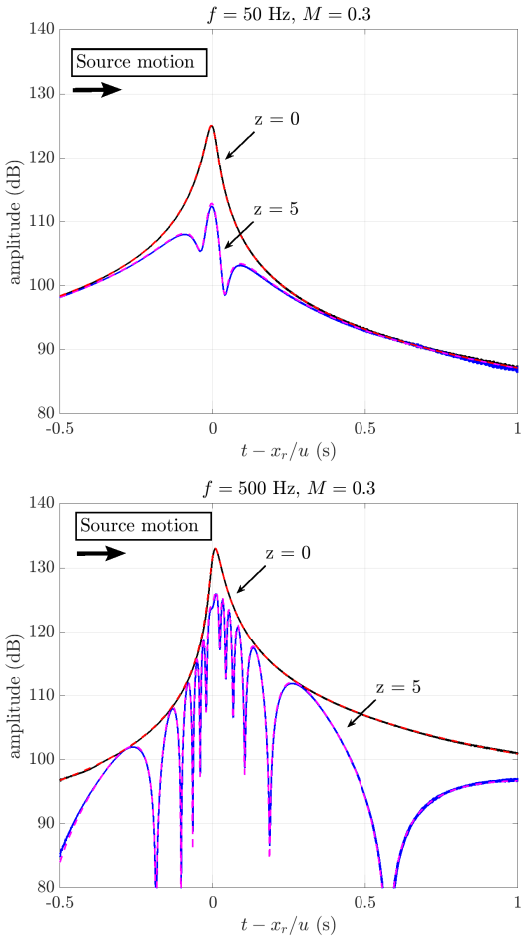

Figure 4. Comparison of the 3D FDTD simulation (black and blue lines) with the heuristic formulation (red and magenta dashed lines) in presence of a *rigid* ground. The source speed is $M = 0.3$ and the frequencies are $f = 50$ Hz (top) and 500 Hz (bottom). Results are shown for two receivers located at $x = 40, y = 0$ m at heights $z = 0$ m and $z = 5$ m.

3.2.2 *Absorbing ground*

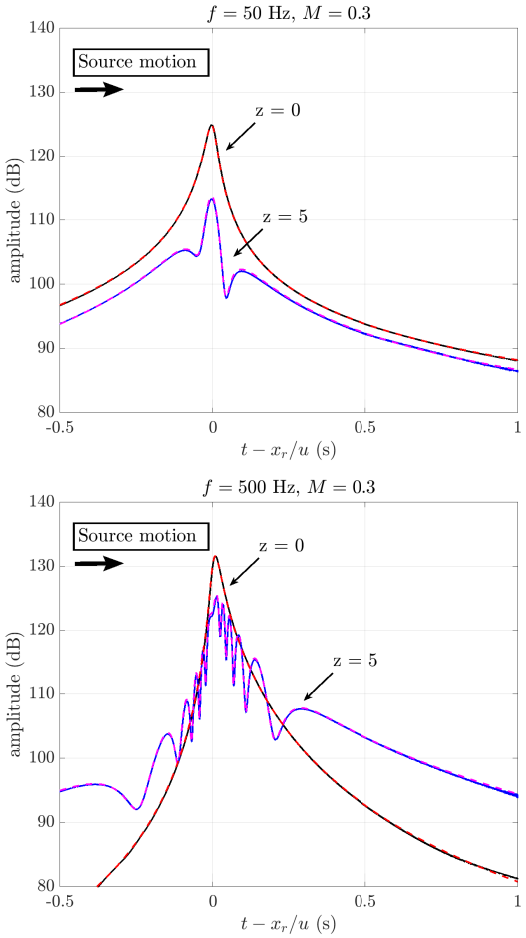

Figure 5. Comparison of the 3D FDTD simulation (black and blue lines) with the heuristic formulation (red and magenta dashed lines) in presence of the *long-grass* ground. The source speed is $M = 0.3$ and the frequencies are $f = 50$ Hz (top) and 500 Hz (bottom). Results are shown for two receivers located at $x = 40, y = 0$ m at heights $z = 0$ m and $z = 5$ m.

Fig. 5 shows also an excellent agreement between the FDTD solution and the heuristic simulations. The same consequences of convective amplification and Doppler effect are noticed. However, compared to rigid ground, the interference patterns are shifted, and the dips are less visible due to the change in ground properties. It should be noted that for grazing angles of incidence for $f = 500$ Hz, a higher amplitude is observed at the receiver (40, 0, 5) m than at the receiver (40, 0, 0) m on the ground.

4. PARAMETRIC ANALYSIS ON GROUND PROPERTIES

This section performs a parametric analysis on ground parameters in the context of aircraft noise certification. A receiver is placed at $(680, 25, 1.2)$ m, and the point source is moving along a slight upward slope $z_s = 0.09x + 296$ m, at constant speed with Mach number $M = 0.2$, as illustrated in Fig. 6. Two types of ground are considered: the *rigid* ground where $\beta = 0$, and the *long-grass* absorbing ground. Results are presented for the three frequencies $f = 50, 500, 2500$ Hz in Fig. 7.

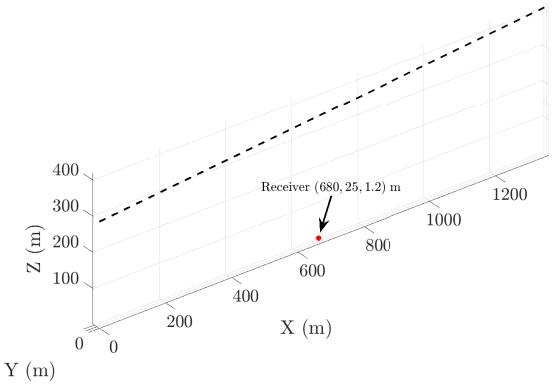

Figure 6. Schematic of the case studied. The point source is moving along an upward slope $z_s = 0.09x + 296$ m, at constant speed $M = 0.2$ (black dashed line). The receiver is located at $(680, 25, 1.2)$ m (red star).

Fig. 7 shows significant differences in sound level (up to several decibels), especially in the interference patterns region for $f = 500$ Hz and $f = 2500$ Hz. The interference patterns dips are much less pronounced and are shifted in time due to the phase effects that differ between the two types of ground. Results also show that for some specific geometrical configuration ($t - x_r/u \approx 0$ at $f = 500$ Hz) the sound levels can be higher with the absorbing ground than with the rigid ground.

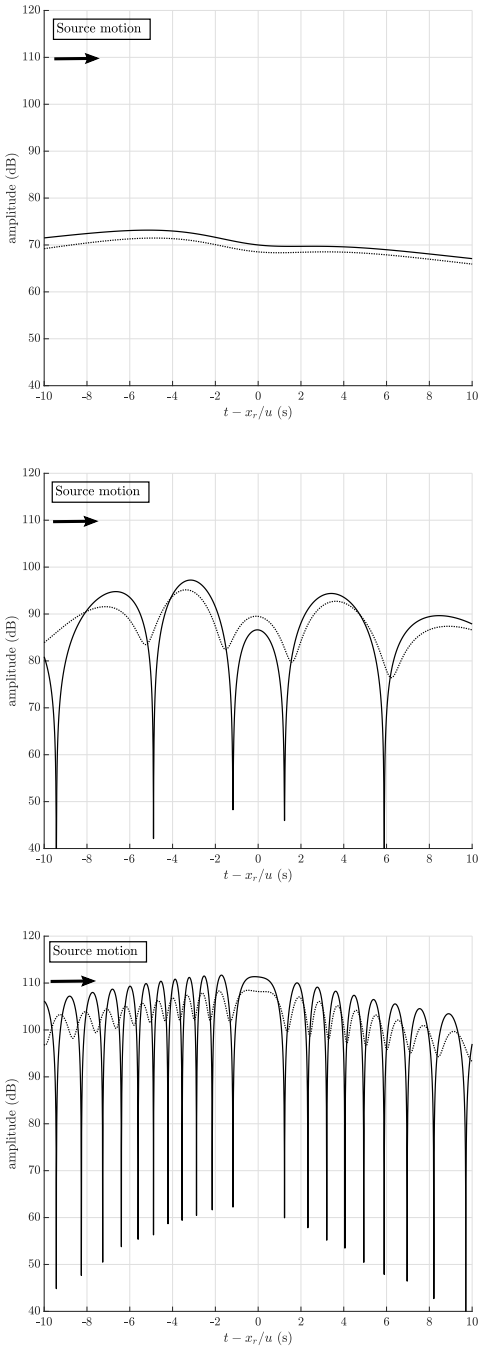

Figure 7. Sound pressure level at the receiver $(680, 25, 1.2)$ m for both *rigid* (solid line) and *long-grass* (dashed line) grounds. The source is moving at $M = 0.2$ along an upward slope. Results are presented for $f = 50$ Hz (top), $f = 500$ Hz (middle) and $f = 2500$ Hz (bottom).

Table 1. Equivalent sound level L_{eq} (dB) at the receiver $(680, 25, 1.2)$ m for both *rigid* and *long-grass* grounds.

	50 Hz	500 Hz	2500 Hz
rigid	71.0 dB	90.9 dB	106.3 dB
long-grass	69.4 dB	89.4 dB	103.8 dB
difference	1.6 dB	1.5 dB	2.5 dB

Finally, Tab. 1 presents the equivalent sound level L_{eq} at the receiver position for the three frequencies considered. The L_{eq} is given by:

$$L_{\text{eq}} = 10 \log_{10} \left[\frac{1}{t_2 - t_1} \int_{t_1}^{t_2} \frac{|p|^2}{p_0^2} \, \mathrm{d}t \right], \qquad (17)$$

where t_1 is the start time, t_2 is the end time and $p_0 = 20$ µPa is the reference pressure. Results also show significant differences between the two ground types, which highlights the need to properly determine the ground effects in aircraft noise certification scenario.

5. CONCLUSION AND PERSPECTIVES

This paper has presented a heuristic formulation of the sound field emitted by a moving point source in a homogeneous atmosphere above an absorbing ground. The formulation has been validated with regard to a 3D FDTD solution that solves the linearized Euler equations. A parametric study on ground parameters has been proposed in order to quantify ground influence on SPL predictions in the context of aircraft noise certification. Results showed significant differences for both instantaneous SPL and equivalent SPL, which highlights the need to precisely determine ground parameters in order to avoid uncertainty on SPL estimation.

The heuristic formulation can be further enhanced by considering atmospheric effects, *i.e.* refraction and scattering, on sound propagation. More advanced statistical methods could then be used to account for environmental parameters effects on SPL predictions in the context of aircraft noise certification.

6. ACKNOWLEDGMENTS

The present work is part of the program MAMBO "Méthodes avancées pour la modélisation du bruit moteur et avion" (Advanced methods for engine and aicraft noise modelling" coordinated by Airbus SAS. It was supported by the DIrection Générale de l'Aviation Civile (DGAC) under the Grant n° 2021-50. This publication was performed within the framework of the LABEX CeLyA (ANR-10-LABX-0060) of Universite de Lyon, within the program "Investissements d'Avenir" (ANR-16-IDEX-0005) operated by the French National Research Agency (ANR). This work was granted access to the HPC resources of PMCS2I (Pole de Modelisation et de Calcul en Sciences de l'Ingenieur et de l'Information) of Ecole Centrale de Lyon and PSMN (Pole Scientifique de Modelisation Numerique) of ENS de Lyon, members of FLMSN (Federation Lyonnaise de Modelisation et Sciences Numeriques), partner of EQUIPEX EQUIP@MESO.

7. REFERENCES

[1] V. P. Blandeau and P. Bousquet, "A new plate design to improve the accuracy of aircraft exterior noise measurements on the ground," in *AIAA AVIATION 2021 FORUM*, p. 2158, 2021.

[2] P. Bousquet and V. P. Blandeau, "Feasibility of determining aircraft certification noise levels using ground plane microphone measurements," in *AIAA AVIATION 2021 FORUM*, p. 2159, 2021.

[3] K. Attenborough, K. M. Li, and K. Horoshenkov, *Predicting outdoor sound*. CRC Press, 2006.

[4] P. M. Morse and K. U. Ingard, *Theoretical acoustics*. Princeton university press, 1968.

[5] T. Norum and C. Liu, "Point source moving above a finite impedance reflecting plane—experiment and theory," *The Journal of the Acoustical Society of America*, vol. 63, no. 4, pp. 1069–1073, 1978.

[6] S. Oie and R. Takeuchi, "Sound radiation from a point source moving in parallel to a plane surface of porous material," *Acta Acustica united with Acustica*, vol. 48, no. 3, pp. 123–129, 1981.

[7] M. Ochmann, "Exact solutions for sound radiation from a moving monopole above an impedance plane," *The Journal of the Acoustical Society of America*, vol. 133, no. 4, pp. 1911–1921, 2013.

[8] K. M. Li and Y. Wang, "On the three-dimensional sound fields from a moving monopole source above a non-locally reacting ground," *The Journal of the Acoustical Society of America*, vol. 147, no. 4, pp. 2581–2596, 2020.

[9] D. Dragna, P. Blanc-Benon, and F. Poisson, "Modeling of broadband moving sources for time-domain simulations of outdoor sound propagation," *AIAA Journal*, vol. 52, no. 9, pp. 1928–1939, 2014.

[10] D. Dragna and P. Blanc-Benon, "Sound radiation by a moving line source above an impedance plane with frequency-dependent properties," *Journal of Sound and Vibration*, vol. 349, pp. 259–275, 2015.

[11] Y. Wang, K. Li, D. Dragna, and P. Blanc-Benon, "On the sound field from a source moving above non-locally reacting grounds," *Journal of sound and vibration*, vol. 464, p. 114975, 2020.

[12] D. Dragna and P. Blanc-Benon, "Towards realistic simulations of sound radiation by moving sources in outdoor environments," *International Journal of Aeroacoustics*, vol. 13, no. 5-6, pp. 405–426, 2014.

[13] M. Buret, *New analytical Models for outdoor moving sources of sound*. Doctoral Dissertation, Open University, 2002.

[14] K. Attenborough and T. Van Renterghem, *Predicting outdoor sound*. CRC Press, 2021.

[15] C. Bogey and C. Bailly, "A family of low dispersive and low dissipative explicit schemes for flow and noise computations," *Journal of Computational physics*, vol. 194, no. 1, pp. 194–214, 2004.

[16] R. Troian, D. Dragna, C. Bailly, and M.-A. Galland, "Broadband liner impedance eduction for multimodal acoustic propagation in the presence of a mean flow," *Journal of Sound and Vibration*, vol. 392, pp. 200–216, 2017.

[17] D. Komatitsch and R. Martin, "An unsplit convolutional perfectly matched layer improved at grazing incidence for the seismic wave equation," *Geophysics*, vol. 72, no. 5, pp. SM155–SM167, 2007.

[18] K. Attenborough, I. Bashir, and S. Taherzadeh, "Outdoor ground impedance models," *The Journal of the Acoustical Society of America*, vol. 129, no. 5, pp. 2806–2819, 2011.